Electronic Supplementary Information

$NiFe_2O_4$, Fe_3O_4–Fe_xNi_y or Fe_xNi_y loaded Porous Activated Carbon Balls as Lightweight Microwave Absorbent

Guomin Li [a,b], Liancheng Wang [a], Wanxi Li [a,b], and Yao Xu [a,*]

[a] Key Laboratory of Carbon Materials, Institute of Coal Chemistry, Chinese Academy of Sciences, Taiyuan 030001, China

[b] University of Chinese Academy of Sciences, Beijing 100049, China

[*] Address for correspondence. E-mail: xuyao@sxicc.ac.cn

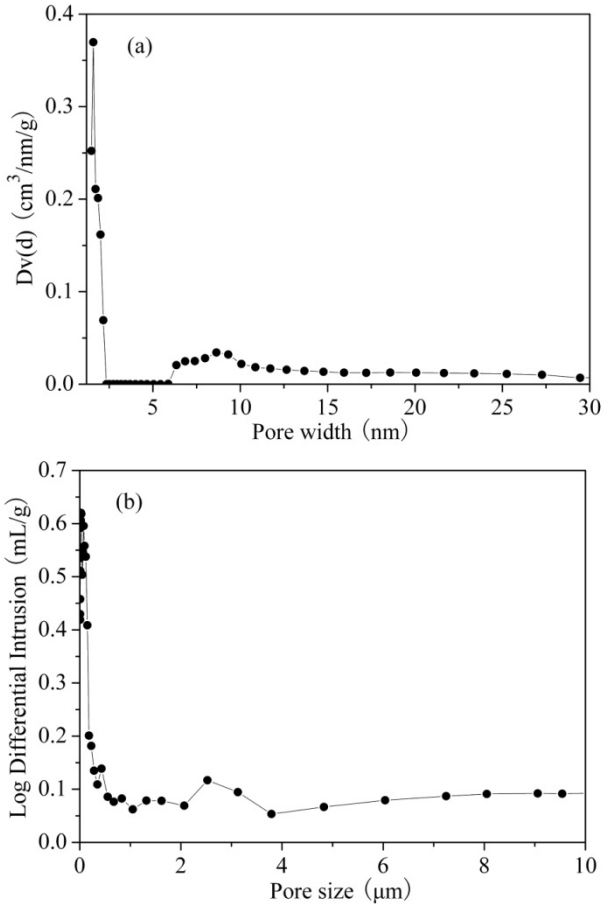

Fig. S1 Pore size distribution of the pristine PACB (a) from the adsorption branches of the isotherms using BJH method, (b) from mercury porosimetry.

Fig. S1a shows the pore size distribution curve of the pristine PACB, calculated from the adsorption branches of the isotherms using BJH method according to density functional theory. The pore size focuses on the range of 1–2.5 nm and 6–12 nm, exhibiting the characteristic of microporosity and mesoporosity. Fig. S1b gives the pore size distribution measured through mercury porosimeter, indicating that the pore is micron size, and its size $d \leq 4$ μm.

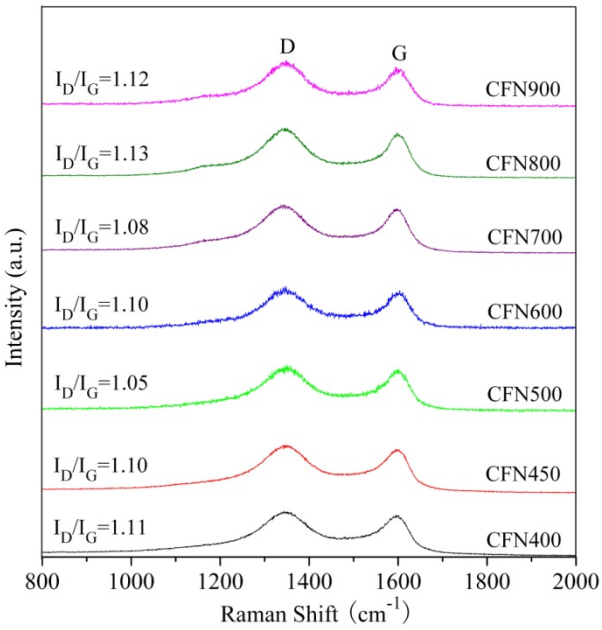

Fig. S2 Normal Raman spectra of PACB composites treated at different temperature.

Fig. S2 gives the typical Raman spectra of CFN400, CFN450, CFN500, CFN600, CFN700, CFN800, and CFN900. The spectra were collected in the range of 800–2000 cm^{-1}, in which two characteristic bands appeared. That is the D peak at around 1350 cm^{-1} and G peak at about 1590 cm^{-1}, which represent the disordered carbon structure and graphite carbon, respectively, and the degree of graphitization can be represented by the relative intensity ratio ($R=I_D/I_G$). It is evident that no obvious change of graphitization was observed after heat treatment compared with 1.11 of the pristine PACB.

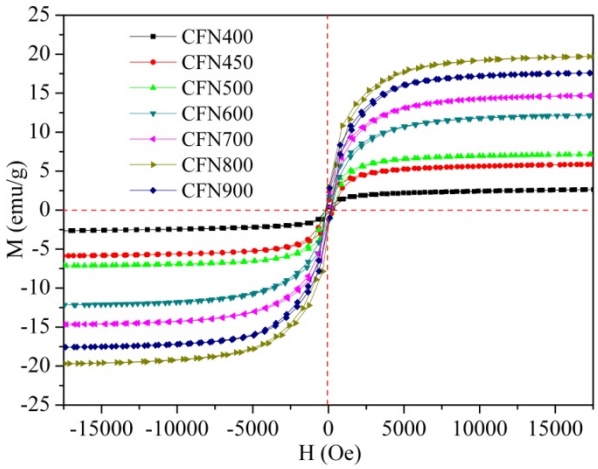

Fig. S3 Magnetic hysteresis loop of the samples measured at room temperature.

Fig. S3 gives the magnetic hysteresis loops of the samples, the magnetization curves show a similar magnetic behavior.

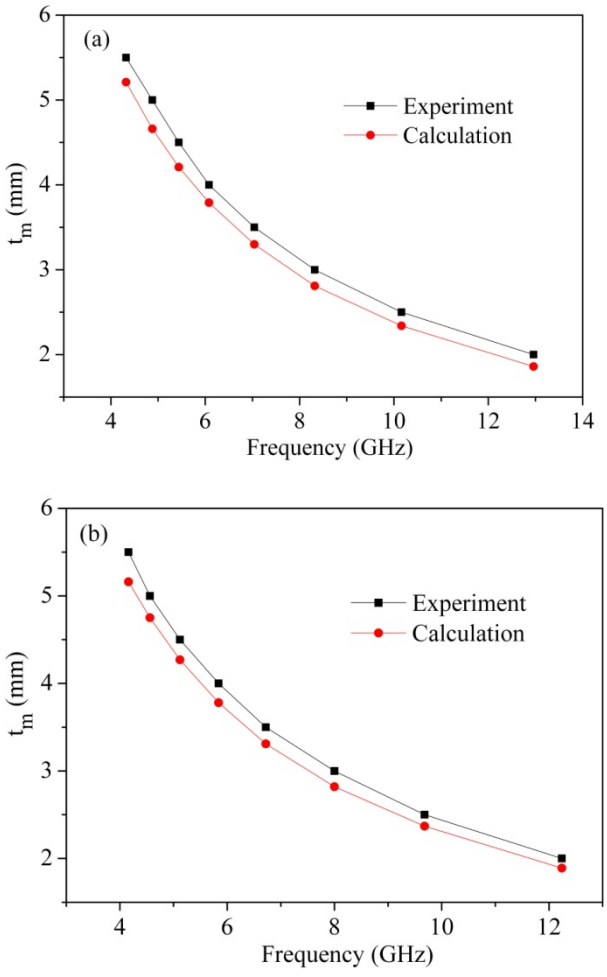

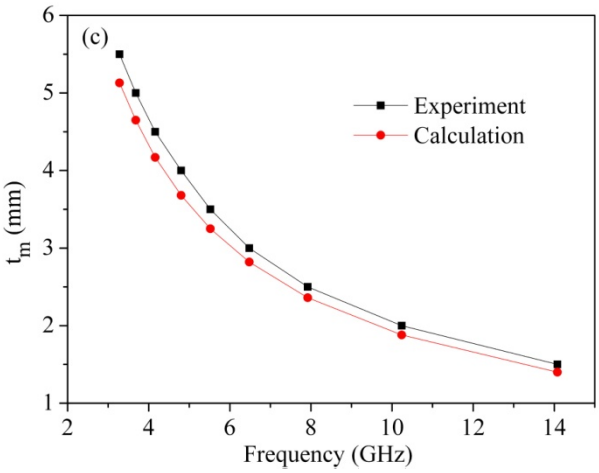

Fig. S4 dependence of λ/4 thickness (calculated and experimental) on frequency for the PACB composites: (a) CFN400, (b) CFN500, and (c) CFN800.

Fig. S4 displays the dependence of $\lambda/4$ thickness on frequency for the PACB composites. After comparing the matching thickness t_m^{cal} calculated by Eq. (9) ($f = f_m$) with the experimental matching thickness t_m^{exp}, it's evident that the calculated result t_m^{cal} agrees well with the experimental value t_m^{exp}.

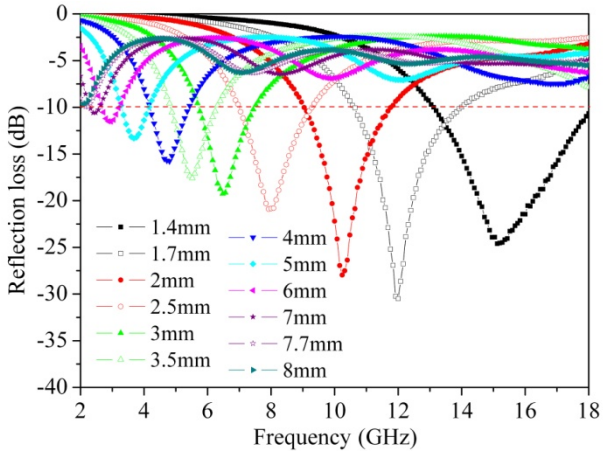

Fig. S5 Microwave RL curves of the CFN800 at different coating thickness.